Neurobiology of Disease 213 (2025) 107014

Contents lists available at ScienceDirect

Neurobiology of Disease

journal homepage: www.elsevier.com/locate/ynbdi

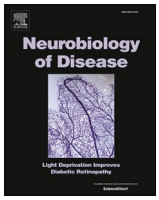

[^{18}F]FDG PET metabolic correlates of cerebrospinal fluid TAR DNA-binding protein 43 in prodromal Alzheimer's disease

Virginia Pelagotti [a,1], Domenico Plantone [b,1], Francesca D'Amico [c], Stefano Raffa [c,d], Pietro Mattioli [a,d], Beatrice Orso [a], Mattia Losa [a], Carlo Manco [b], Delia Righi [b], Dario Arnaldi [a,d], Antonio Uccelli [a,d], Andrea Chincarini [e], Gianmario Sambuceti [c,d], Silvia Morbelli [f,g], Nicola De Stefano [b], Federico Massa [a,d,2], Matteo Pardini [a,d,*,2]

[a] Department of Neuroscience, Rehabilitation, Ophthalmology, Genetics, Maternal and Child Health (DINOGMI), University of Genoa, Genoa, Italy
[b] Department of Medicine, Surgery, Neuroscience, University of Siena, Siena, Italy
[c] Department of Health Science (DISSAL), University of Genoa, Italy
[d] IRCCS Ospedale Policlinico San Martino, Genoa, Italy
[e] National Institute of Nuclear Physics (INFN), Genoa section, Genoa, Italy
[f] Department of Medical Science, Università degli studi di Torino, Turin, Italy
[g] Nuclear Medicine Unit, Città della Salute e della Scienza di Torino, Turin, Italy

ARTICLE INFO

Keywords:
Alzheimer's disease
LATE
FDG-PET
TDP-43

ABSTRACT

Introduction: Limbic-predominant age-related TDP-43 encephalopathy neuropathological changes (LATE-NC) are characterized by phosphorylated TDP-43 aggregates in limbic regions, often co-occurring with Alzheimer's disease (AD) pathology, amplifying clinical and neuroimaging alterations. *In vivo* biomarkers for LATE-NC are lacking, but changes in CSF TDP-43 levels may reflect LATE-NC in AD patients. This study explored the correlation between CSF TDP-43 and [^{18}F]FDG PET metrics in prodromal AD, providing insights into the impact of LATE-NC on AD brain metabolism.

Methods: We measured CSF TDP-43 levels using an ultrasensitive immunoassay in 27 MCI-AD patients. To analyze brain metabolism, we employed both a volume of interest (VOI)-based approach and a voxel-based analysis (VBA) of [^{18}F]FDG PET scans. The VOI-based approach focused on metabolic values from regions associated with LATE-NC, such as the inferior (IT) and medial temporal (MT) regions, in previous studies. Through VBA, we explored the CSF TDP-43-related brain regions and their spatial association with relative hypometabolism compared with 40 healthy controls (HC), adjusting for relevant covariates.

Results: CSF TDP-43 levels directly correlated with metabolism in the temporo-parietal cortex, particularly the bilateral precuneus, and showed spatial independence from relative hypometabolic areas. The VOI analysis revealed no significant correlations between TDP-43 and the MT-VOI, IT-VOI, or their ratio.

Conclusions: TDP-43 pathology in prodromal AD, as indicated by elevated CSF TDP-43 levels, contributes to metabolic disruptions in posterior parietal regions, particularly the precuneus. These changes diverge from typical amyloid- and tau-related alterations, offering indirect *in vivo* insights into TDP-43 co-pathology in prodromal AD.

1. Introduction

Transactive response DNA-binding protein of 43 kDa (TDP-43) is an essential intranuclear protein for gene expression, RNA splicing, and metabolism. In pathological conditions, TDP-43 undergoes post-translational modifications like ubiquitination and phosphorylation, leading to cytoplasmic aggregation. These aggregates, are hallmark pathological features of amyotrophic lateral sclerosis (ALS),

* Corresponding author at: Department of Neuroscience, Rehabilitation, Ophthalmology, Genetics, Maternal and Child Health (DINOGMI), University of Genoa, Largo Daneo 3, 16132 Genoa, Italy.
E-mail address: matteo.pardini@unige.it (M. Pardini).
[1] Equally contributing as first authors.
[2] Equally contributing as last authors.

https://doi.org/10.1016/j.nbd.2025.107014
Received 19 February 2025; Received in revised form 13 June 2025; Accepted 30 June 2025
Available online 1 July 2025

frontotemporal lobar degeneration with ubiquitin inclusions (FTLD-TDP), and limbic-predominant age-related TDP-43 encephalopathy neuropathological changes (LATE-NC) (Nelson et al., 2019; Neumann et al., 2021). TDP-43 aggregates are also observed in a subset of subjects with 4R-tauopathies, Lewy body disease, Alzheimer's disease (AD), as well as in cognitively normal aging as a contributing factor to neurodegeneration. In AD, TDP-43 pathology affects up to 57 % of patients, primarily in limbic brain regions, with progression from the amygdala to the hippocampus and adjacent cortices (Meneses et al., 2021), atrophy and cognitive decline (Butler Pagnotti et al., 2023; Josephs et al., 2017).

Assessment of TDP-43 pathology *in vivo* is challenging, due to the lack of specific biomarkers. TDP-43 concentrations in biofluids have shown conflicting results in ALS and FTLD-TDP, with some studies reporting increased or decreased cerebrospinal fluid (CSF) levels (Kapaki et al., 2022a; Kuiperij et al., 2016), while remains controversial (Foulds et al., 2009). The issue is further complicated in AD, as available data on TDP-43 levels are restricted to plasma, and comparisons with controls and patients with FTLD remain contentious (Bauer et al., 2023; Foulds et al., 2009).

Recent findings by (Bauer et al., 2023), using morphological imaging in older adults, show that higher plasma TDP-43 levels are linked to reduced entorhinal cortex volume and thinner cortical thickness in the cingulate/parahippocampal gyrus, postulating their ability to reflect aggregate accumulation in these regions. CSF TDP-43 may better correlate with TDP-43 pathology with less systemic influences. Indeed, plasma levels can be influenced by systemic factors as circulating TDP-43 is enriched in platelets, fibroblasts, and pancreatic β-cells (Araki et al., 2019; Luthi-Carter et al., 2024; Rubio et al., 2022). Although, low concentrations in CSF hinder detection *via* standard immunoassays (Feneberg et al., 2014). This can be addressed by ultra-sensitive immunoassays such as Simoa technology, which detects both full-length and C-terminal truncated forms of TDP-43, the latter being more prone to aggregation (López-Carbonero et al., 2024). However, quantifying protein levels in biofluids lacks information on the topography of TDP-43 aggregates, which is critical for understanding co-pathology in AD. Few studies have integrated fluid biomarkers with imaging to explore the effects of LATE-NC on neurodegeneration. For example, [^{18}F]FDG PET has been used as an *antemortem* tool to study TDP-43 pathology in patients with AD neuropathological changes (ADNC), following neuropathological confirmation. Buciuc et al., 2020 found that metabolic dysfunction in the medial temporal and frontal regions was significantly associated with TDP-43 burden, particularly in hippocampal sclerosis. Lavrova et al., 2024 observed similar metabolic alterations in patients with low-intermediate ADNC or PART (Primary Age-Related Tauopathy) and pathological LATE-NC. In these patients, visual analysis of *antemortem* imaging revealed a higher likelihood of hippocampal sclerosis and medial temporal lobe atrophy on MRI, along with more pronounced hypometabolism in these regions on [^{18}F]FDG PET, compared to TDP-43-negative cases.

In previous studies, we demonstrated how voxel-based analysis of [^{18}F]FDG PET imaging provides topographical insights into the metabolic correlates of CSF proteins related to synaptopathy or neuronal damage in AD (Massa et al., 2024, 2022). This leverages the ability of [^{18}F]FDG PET to reflect molecular alterations driving neuronal loss and dysfunction in connected regions. In the same perspective, this study the association between CSF TDP-43 levels and regional brain [^{18}F]FDG uptake in patients with MCI due to AD.

To achieve this, we use both a ROI-based approach targeting regions previously associated with LATE-NC, such as the inferior and medial temporal regions (Botha et al., 2018; Buciuc et al., 2020), and a whole-brain voxel-based analysis exploration without predefined hypotheses. Identifying brain regions where CSF TDP-43 levels intersect with metabolic changes may offer valuable *in vivo* insights into the relationship between AD and TDP-43 proteinopathies, particularly in the early, prodromal stages. This approach may underscore regional metabolic alterations as potential biomarkers of TDP-43 pathology, complementing previous studies.

2. Methods

2.1. Patients

We studied a retrospective cohort of 27 patients with typical, high-likelihood MCI-AD (Albert et al., 2011), extracted from an in-house database of 160 patients diagnosed from May 2017 to April 2021. Initial assessments including neurological and neuropsychological examinations, revealed a measurable cognitive impairment with an amnestic profile exceeding age- and education-adjusted norms while preserving abilities in functional and instrumental activities of daily living and not meeting criteria for dementia (Clinical Dementia Rating, CDR = 0.5). We ruled out patients with a non–amnestic presentation while blood tests and brain MRI excluded other MCI etiologies as recommended (Frisoni et al., 2024). As for selection criteria, participants were required to have undergone, at baseline, both i) core AD CSF biomarker assessment (amyloid-beta 1-42/1-40 ratio, Aβ42/40, Tau phosphorylated at threonine-181, pTau181, and total-Tau, tTau), indicating an AD-compatible AT(N) profile (Jack et al., 2018), and ii) an [^{18}F]FDG PET scan demonstrating the characteristic temporo-parietal hypometabolism of AD (Morbelli et al., 2015). The two diagnostic biomarker assessments were performed, on average, within a two-month interval. An indispensable requirement was also a clinical follow-up lasting a minimum of 2 years. Eleven patients progressed to typical AD dementia (CDR = 1) after a mean of 1.3 ± 0.6 years from baseline (progressors; pMCI-AD), while 16 remained at the MCI stage after 2.9 ± 1.1 years (range 0.5–2.76 years) (non-progressors; npMCI-AD).

All study procedures were performed during clinical practice. All patients provided informed consent for the use of clinical data for research purposes on the association between markers of neurodegeneration. All study procedures were performed according to the declaration of Helsinki.

2.2. CSF biomarkers collection and analysis

CSF (10–12 mL) was collected in sterile tubes after an overnight fast, then centrifuged and stored at −80 °C until analysis. The Lumipulse G600 II® system (Fujirebio Europe, Gent, Belgium) measured core AD biomarkers for diagnostic purpose with in-laboratory validated assay cartridge cut-offs: Aβ42/40 ratio 0.069, pTau181 56.5 pg/mL, t-Tau 404 pg/mL biomarkers (Massa et al., 2024, 2022).

For CSF TDP-43 quantification, a commercially available immunoassay kit (Catalog#103293; Quanterix, Billerica, MA, USA) was used with the semi-automated ultrasensitive SR-X Biomarker Detection System. The assay targeted amino acids 203–209 and the C-terminal region of TDP-43, detecting both full-length and truncated forms in diluted samples (1:40). No validated cut-offs currently exist in the literature for the CSF TDP-43 Simoa assay.

Protein concentrations were measured in pg/mL. Quality control samples exhibited concentrations within the predefined range (<10 % coefficient of variance across plates). Spearman's partial correlation analysis of CSF biomarkers, both unadjusted and adjusted for age, was performed using R Statistical Software (v4.3.3), with significance set at $p < 0.05$.

2.3. [^{18}F]FDG PET imaging acquisition, pre-processing and analysis

The methodology for acquisition and image pre-processing is detailed in prior research (Massa et al., 2024, 2022) and in supplementary materials.

2.4. Statistical analysis

2.4.1. Clinical-demographical data and CSF biomarkers

Normality of clinical-demographic variables and CSF biomarker values was assessed with the Shapiro–Wilk test. Because the distributions deviated from normality, subgroup comparisons (npMCI-AD *vs* pMCI-AD) were conducted using the Wilcoxon rank-sum test. Spearman partial correlations among CSF biomarkers were computed both unadjusted and adjusted for age. All analyses were performed in Jamovi Statistical Software (version 2.3) with a two-tailed significance threshold of $p < 0.05$.

2.4.2. Voxel-based analysis (VBA)

Following preprocessing, the smoothed images underwent a voxel-wise group analysis (Statistical Parametric Mapping, SPM12), exploring the whole brain without any *a priori* hypothesis of involved brain regions, including:

1) two-sample *t*-test comparing the scans of the patients and a healthy control (HC) group of 40 age-, sex- and education-matched volunteers (Massa et al., 2024, 2022), with age and MMSE as confounders. In HC, eligibility required: (i) intact general health confirmed by clinical history and examination; (ii) normal cognition (MMSE > 27; CDR = 0); and (iii) a normal FDG-PET pattern independently verified by two expert nuclear-medicine physicians."

   Relatively hypometabolic regions in patients were labelled as AD-related volumes of interest (AD-VOIs).
2) multiple linear regression analysis to identify a TDP-43-VOI using [^{18}F]FDG brain metabolism as dependent variable, CSF TDP-43 values as covariate, age and MMSE as confounders. Additionally, CSF pTau181 as a confounder was incorporated for exploratory purposes. Voxel values were normalized according to cerebellar cortex activity following the approach described in previous work (Massa et al., 2024). This normalization enhances the detection of cortical abnormalities by leveraging the unaffected cerebellum in neurodegenerative conditions such as AD. CSF TDP-43 values were log-transformed due to right-skewed distribution ($p < 0.001$, Lilliefors test), enabling linear models. The analysis was conducted exclusively on the MCI-AD group.

A 0.8 grey matter threshold mask and $p < 0.001$ height threshold without multiple comparison correction at voxel-level were applied in all analyses. Clusters≥100 voxels were considered significant at $p < 0.05$ FWE-corrected for multiple comparisons at cluster-level. Cluster coordinates were processed using GingerALE and Talairach Client software to align them with the Brodmann-classified Talairach 3D atlas.

2.4.3. Volume of interest (VOI)-analysis

Using the Marsbar (MARSeille Boîte À Région d'Intérêt) toolbox implemented in SPM12, we computed the average count density of distinct VOIs, scaled against the cerebellar cortex as a reference, to correlate with CSF TDP-43 levels for each MCI-AD patient. Precisely, in addition to the TDP-43-VOI identified in the previous VBA, we analyzed regions selected *a priori* from previous studies (Botha et al., 2018; Buciuc et al., 2020) as critical for AD-associated TDP-43 proteinopathy. These included the inferior temporal gyrus (IT), which is relatively preserved in LATE-NC compared to the medial temporal lobe (MT), encompassing the amygdala and hippocampus.

The resulting counts of the TDP-43-VOI, IT and MT VOIs - analyzed either independently or as an IT-to-MT ratio (IMT ratio) following (Botha et al., 2018) - were correlated with each other and with CSF TDP-43 levels using Spearman analysis, both unadjusted and partially adjusted for age.

2.4.4. Voxel-wise inter-regional correlation analysis (IRCA)

The cerebellum-scaled average count density values of the TDP-43-VOI were utilized as a covariate in an inter-regional correlation analysis (IRCA) to identify brain regions showing significant voxel-wise correlations with the TDP-43-VOI itself. This approach is widely employed to map resting-state metabolic connectivity by assessing voxel-wise correlations between a predefined volume of interest (VOI) and all other brain voxels. Strong correlations indicate regions functionally connected to the VOI, which can be interpreted as part of a shared metabolic network. Here, this method was applied to determine whether the TDP-43-VOI acts as a central hub within a specific pathological network relevant to early AD. This analysis was conducted separately for the MCI-AD and HC groups, following the validated procedure by (Lee et al., 2008) and previously applied in MCI-AD patients (Kreshpa et al., 2024; Massa et al., 2020). The criteria for the analysis outputs and the extraction of cluster coordinates were consistent with those described earlier.

3. Results

3.1. Clinical-demographical data and CSF biomarkers

Clinical-demographic characteristics and CSF biomarker values are reported in Table 1. The only statistically significant difference between the npMCI-AD and pMCI-AD subgroups was the baseline MMSE score ($p = 0.039$), as expected. No other significant differences—including CSF biomarker levels—were detected.

Moreover, there was no significant correlation between CSF levels of TDP-43 and core AD CSF markers. Conversely, we observed a highly significant positive correlation between CSF levels of pTau181 and t-Tau ($r = 0.94$, $p < 0.001$), as expected (Supplementary Table 1s).

3.2. [^{18}F]FDG PET statistical analysis

3.2.1. Voxel-based analysis (VBA)

Three relatively hypometabolic AD-VOIs encompassed the temporo-parietal regions and marginally involved the frontal lobe in the right hemisphere. We observed a significant direct correlation of CSF TDP-43 with brain metabolism in posterior parietal regions, particularly in bilateral precuneus (TDP-43-VOI). The incorporation of pTau181 as a confounder did not materially alter the finding (data not shown).

Table 2 details extension, coordinates, and corresponding Brodmann areas of the VOIs, which are displayed in Fig. 1.

Table 1
Main clinical characteristics and CSF biomarkers levels in MCI-AD patients.

Demographical and clinical variables	MCI-AD	npMCI-AD	pMCI-AD	*p*-Value
Age (years)	74.1 ± 5.9	74.4 ± 3.6	73.6 ± 8.4	0.865
Sex (M:F)	7:20	4:12	3:8	>0.999
MMSE score	25.4 ± 2.9	26.4 ± 1.9	24.0 ± 3.4	**0.039**
Education (y)	10.4 ± 4.6	10.7 ± 4.2	9.6 ± 5.4	0.295
CSF biomarkers				
CSF Aβ42/Aβ40 ratio	0.043 ± 0.010	0.048 ± 0.10	0.10 ± 0.2	0.198
CSF pTau181 (pg/ml)	125.4 ± 72.4	120.9 ± 69.0	131.9 ± 80.0	0.837
CSF t-Tau (pg/ml)	796.1 ± 446.8	764.6 ± 442.8	842.1 ± 470.0	0.544
CSF TDP-43 (pg/ml)	38.8 ± 33.2	30.4 ± 23.6	51.0 ± 41.8	0.178

Mean ± SD and *p* value are shown. Significant results in bold.
Abbreviations: MCI-AD, Mild cognitive impairment due to Alzheimer's disease; np, non-progressors; p, progressors; F, female; M, male; MMSE, Mini Mental State Examination; CSF, Cerebrospinal fluid; Aβ42/Aβ40 ratio, amyloid Aβ1–42 normalized for amyloid Aβ1–40; pTau181, Tau phosphorylated at threonine 181; t-Tau, total Tau; TDP-43, TAR DNA-binding protein 43; SD, standard deviation.

Table 2
Significant brain areas resulting from the voxel-wise group analysis.

Extension (number of voxels)	X	Y	Z	Cortical region (gyrus)	BA
Hypometabolism in MCI-AD with respect to HC group (AD-VOIs)					
2798	43.5	−37.9	−13.0	Fusiform R	–
(AD1-VOI)	43.6	−30.1	−15.9	Fusiform R	–
	47.2	−39.8	−13.1	Fusiform R	–
	43.8	−4.8	−24.3	Fusiform R	–
	46.5	−59.2	31.9	Angular R	–
	47.4	5.3	−12.4	Superior Temporal R	–
	29.8	−67.1	36.3	Precuneus R	31
	45.6	7.5	−15.9	Superior Temporal R	–
	41.1	−67.6	22.0	Middle Temporal R	–
	43.0	−67.1	16.7	Middle Temporal R	–
1329	7.7	−64.4	28.9	Precuneus R	31
(AD2-VOI)	9.7	−53.9	17.4	Posterior Cingulate R	–
	−7.1	−65.8	25.0	Precuneus R	31
	13.1	−59.9	40.3	Precuneus R	31
	20.5	−52.8	44.7	Precuneus R	31
704	33.6	3.0	50.2	Middle Frontal R	6
(AD3-VOI)	13.2	8.4	53.9	Superior Frontal R	6
	30.0	16.9	42.4	Middle Frontal R	8
	15.0	−8.4	52.4	Medial Frontal R	6
	24.2	2.2	59.0	Middle Frontal R	6
	26.2	18.1	49.7	Superior Frontal R	6
	24.2	7.4	63.0	Superior Frontal R	6
Correlation with TAR DNA-binding protein 43 levels (TDP-43-VOI)					
785	7.4	−49.7	51.9	Precuneus R	7
(TDP-43-VOI)	−3.8	−48.5	59.1	Precuneus L	7
	14.7	−45.2	63.3	Postcentral R	–
	7.3	−54.3	60.5	Precuneus R	7
	9.2	−54.0	57.0	Precuneus R	7
	−13.0	−46.4	57.3	Precuneus L	7
	22.2	−39.1	58.6	Superior Parietal Lobule R	5
	−16.8	−54.4	61.9	Superior Parietal Lobule L	7
	24.0	−38.0	66.0	Postcentral R	–
	11.4	−46.3	36.1	Precuneus R	31
	5.7	−43.4	45.3	Precuneus R	31
	5.5	−43.1	61.5	Paracentral Lobule R	5

Coordinates and cortical regions in each VOI are ordered downwards from the highest peak *Z*-score.
Abbreviations: BA, Brodmann area; HC, healthy controls; MCI-AD, Mild cognitive impairment due to Alzheimer's disease; VOI, volumes of interest; DIS-VOI, disease-related-VOI; TDP-43, TAR DNA-binding protein 43; IRCA, inter-regional correlation analysis, R, right; L, left, HC, healthy control.

3.2.2. *VOI-based analysis (VOI)*

The Spearman's rank analysis in the MCI-AD group revealed a strong positive correlation between the CSF TDP-43 levels and the TDP-43-VOI counts (unadjusted correlation $r = 0.76$, $p < 0.001$, after correction for age $r = 0.78$, $p < 0.001$), consistent with the results of the VBA. TDP-43 and TDP-43-VOI showed no significant correlations with the other VOIs (*i.e.*, MT-VOI, IT-VOI) or the IMT ratio bilaterally (Supplementary Table 2 and Supplementary Fig. 1s).

3.2.3. *Voxel-wise inter-regional correlation analysis (IRCA)*

In the MCI-AD group, the IRCA revealed that the TDP-43-VOI whole brain-scaled count densities significantly correlated with metabolism in occipital regions (lingual and middle occipital gyri, and cuneus) and cerebellum bilaterally. In the HC group, the TDP-43-VOI whole brain-scaled count densities revealed two significant clusters of correlation, including i) bilateral occipital regions (lingual gyrus and cuneus), and ii) the right striatum and left red nucleus.

The extent (number of voxels), coordinates, and Brodmann areas of the significant clusters resulting from the IRCA analyses, are summarized in Supplementary Table 3s and displayed in Fig. 2.

4. Discussion

Our study revealed a significant positive correlation between CSF TDP-43 levels, measured using the highly sensitive Simoa assay, and metabolic activity in the posterior parietal cortex, primarily the precuneus, in patients with MCI due to AD. This finding is notable given the limited data in the current literature on the use of CSF TDP-43 as a biomarker for TDP-43 neuropathological changes (LATE-NC). Although the interpretation of these results needs caution due to uncertainties about whether CSF TDP-43 levels directly reflect brain aggregate burden, our findings offer valuable insights into the potential impact of TDP-43 proteinopathy in prodromal AD.

The precuneus, a key region within the default mode network (DMN), is involved in self-referential thought, memory retrieval, and higher-order cognitive functions. It is among the first regions to show functional and metabolic changes in AD, even at the early prodromal stage of MCI. Disruptions in connectivity within the DMN are thought to contribute to the cognitive impairments seen in AD, particularly in memory and spatial orientation domains (Buckner and DiNicola, 2019). A pivotal observation from our study is that the metabolic alterations in the TDP-43-VOI appear to be relatively independent of the hypometabolic regions identified in patients with MCI-AD compared to healthy controls, namely the AD-VOIs. This suggests that TDP-43 pathology, as reflected in the TDP-43-VOI, impacts metabolic activity in a manner distinct from the broader metabolic deficits associated with 'pure' AD pathology. This relative independence is further supported by our analysis of correlations between CSF biomarkers, where CSF TDP-43 levels were not significantly associated with core AD biomarkers, such as amyloid-β and tau proteins. These findings imply that TDP-43 pathology may follow a spatially separate pathway from the hallmark amyloid and tau pathologies of AD, as a partly independent driver introducing unique disruptions within functional and metabolic networks already predominantly affected by AD. Alternatively, synergistic TDP-43 proteinopathy and Alzheimer's neuropathology in limbic regions may underlie this outcome. In a large neuropathological cohort of individuals with AD, the presence of TDP-43 in the hippocampus was linked to higher rates of hippocampal atrophy (Josephs et al., 2017), with the strongest association in individuals with moderate-to-high likelihood of AD and neurofibrillary tangles (NFTs) Braak stages III-IV. Moreover, both pathologies tend to originate in limbic regions, follow comparable spreading patterns, and frequently colocalize and interact in AD and FTLD-TDP in tissue (Josephs et al., 2017; Nelson et al., 2019; Tomé et al., 2021). Consistent with this, the presence of TDP-43 aggregates in AD appears to lower the threshold for dementia, amplifying both neuroimaging abnormalities and clinical severity (Josephs et al., 2017). However, we cannot suggest that the metabolic association with the precuneus region involved in the TDP-43-VOI reflects a mere downstream consequence of hippocampal pathology. Indeed, hippocampal functional connectivity is primarily observed in the more ventral parts of the posterior medial cortex, particularly in the retrosplenial posterior cingulate (Rolls et al., 2023). This explains the typical metabolic pattern of AD (Morbelli et al., 2015), which is linked to the disconnection between the parietal and cingulate regions and the hippocampal/entorhinal regions (Matsuda, 2001). These areas are affected in the early stages due to neurofibrillary tangles (NFTs) secondary to cerebral amyloid accumulation (Braak et al., 2006). On the other hand, the posterior precuneus, which is encompassed by the TDP-43-VOI and as part of the DMN, is involved in integrating visual, spatial, and self-related information with the occipital regions, which are critical for visual processing (Buckner and DiNicola, 2019; Rolls et al., 2023). Notably, adjusting for CSF pTau181, a marker of amyloid-related Tau pathology, did not materially change the results of the voxel-based correlation analysis of CSF TDP-43 with brain [^{18}F]FDG uptake. If co-varying tau pathology had driven the association, controlling for pTau181 would have weakened or abolished the TDP-43 correlation with posterior parietal metabolism. Instead, the persistent relationship further demonstrates that

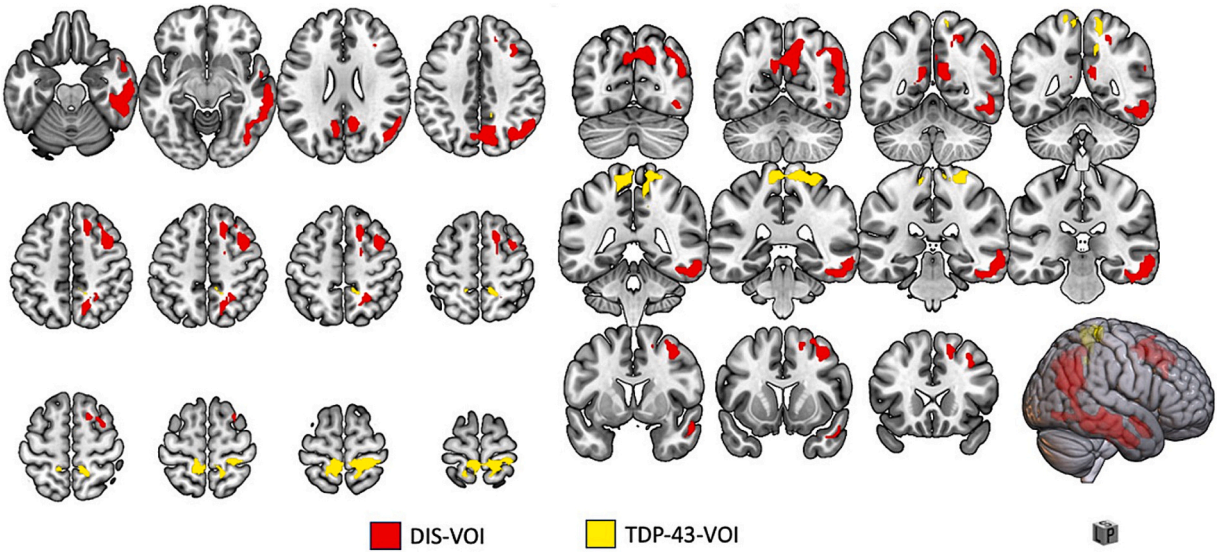

Fig. 1. The two-dimensional representation (axial cuts on the left, coronal on the right) and three-dimensional rendering depict the metabolic correlate of TDP-43 (TDP-43-VOI) (in yellow), overlaid on the MNI reference atlas using MRIcroGL software). Its spatial relation to AD-VOI (in red), formed by the three clusters derived from the comparison between MCI-AD and HC groups, can be visually assessed.
Abbreviations: VOI, volume of interest, AD-VOI, Alzheimer's disease related VOI, TDP-43, TAR DNA-binding protein 43 related VOI. (For interpretation of the references to color in this figure legend, the reader is referred to the web version of this article.)

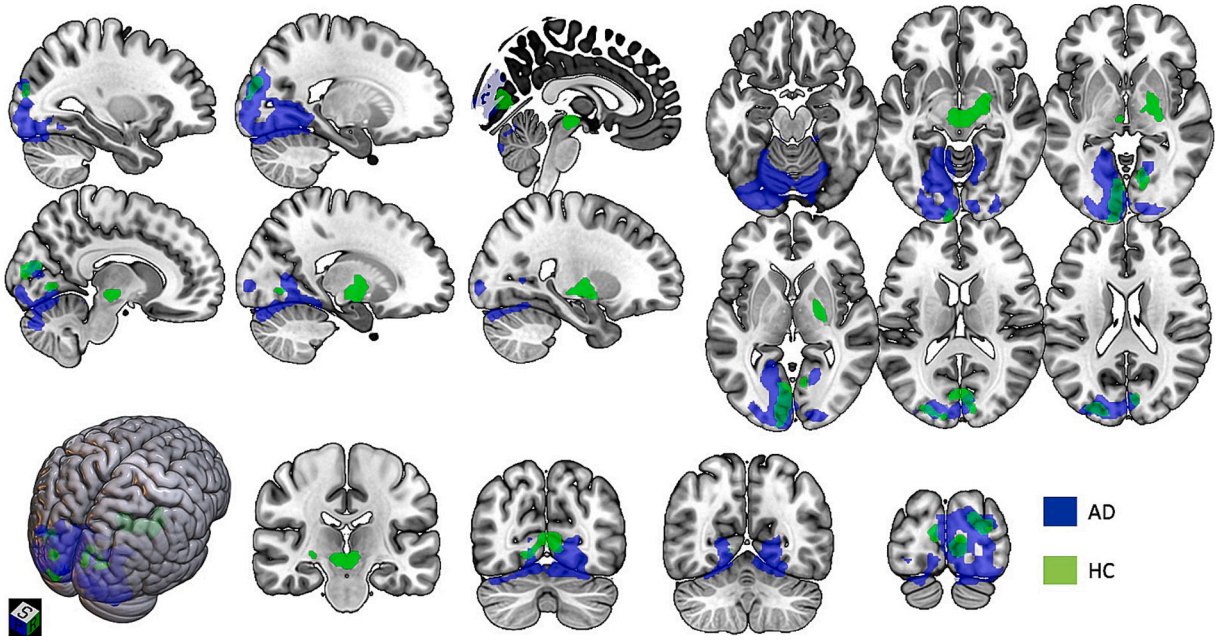

Fig. 2. The two-dimensional representation (axial, coronal and sagittal cuts) and three-dimensional rendering depict the voxel-wise inter-regional correlation analysis (IRCA) of the TDP-43-VOI in the MCI-AD (in blue) and HC (in green), overlaid on the MNI reference atlas using MRIcroGL software.
Abbreviations: VOI, volume of interest, AD-VOI, Alzheimer's disease related VOI, TDP-43, TAR DNA-binding protein 43 related VOI. (For interpretation of the references to color in this figure legend, the reader is referred to the web version of this article.)

TDP-43 co-pathology exerts its metabolic effects largely independently of tau burden in AD. The results from our additional inter-regional correlation analysis (IRCA) using the TDP-43-VOI as a seed region and revealing interconnections between the precuneus and occipital regions, are consistent with this functional profile. Moreover, the IRCA revealed a distinct functional connectivity pattern in HC compared to MCI-AD patients. Noteworthy, IRCA maps for the two groups were compared qualitatively, following the atlas-based overlay method used in our earlier studies (Kreshpa et al., 2024; Massa et al., 2020), with no inferential statistics. Their primary purpose was to illustrate that metabolic connectivity of TDP-43 VOI is confined to parieto-occipital circuitry and spares the medial temporal lobe. We noted, qualitatively, that connectivity anchored to the TDP-43 VOI is already attenuated in prodromal AD. Precisely, in HC, the TDP-43-VOI showed connectivity with deep brain structures, particularly the striatum, which was absent in MCI-AD patients. This alteration in connectivity may reflect early disruptions in the integration of cortical and subcortical systems, contributing to cognitive impairments as observed in prodromal AD (Seoane et al., 2024). However, HC–patient contrasts should be viewed as exploratory and fall outside the primary scope of the IRCA analysis, because of the

different sources in metabolic variance of HC and MCI-AD, namely aging and AD-related neurodegeneration, respectively.

Previous authors reported of significant metabolic dysfunction in the medial temporal and frontal regions associated with TDP-43 burden and hippocampal sclerosis (Buciuc et al., 2020). Particularly, they used the Inferior-to-Medial Temporal (IMT) ratio derived from [^{18}F]FDG uptake, a measure previously described by (Botha et al., 2018) as a proxy of hippocampal sclerosis and LATE-NC. Our attempt to apply a ROI-based approach correlating *a priori* CSF TDP-43 and metabolic values from regions previously associated with LATE-NC, such as the inferior and medial temporal regions as well as their IMT ratio, did not yield significant results. This negative finding is unsurprising in our biomarker-confirmed AD cohort, where CSF TDP-43 is expected to modulate metabolism mainly within parieto-occipital circuits already compromised by Alzheimer's pathology, rather than to drive limbic or inferior-frontal dysfunction as observed in tau-negative or hippocampal-sclerosis cases as in Botha et al. (2018). It is important to note that these VOIs were derived from studies comparing pre-mortem neuroimaging data in patients with confirmed autopsy diagnoses of TDP-43 proteinopathy (Botha et al., 2018; Buciuc et al., 2020), suggesting a more advanced neuropathological stage in those patients, compared to our sample. Indeed, Buciuc et al. (2020) evaluated 73 autopsy-confirmed AD-spectrum cases, but only 11 (three TDP-43-positive and eight TDP-43-negative) were at the MCI stage, and the mean age exceeded 80 years. Therefore, both TDP-43 and AD pathology were probably more advanced than in our younger MCI-AD cohort. Instead, our voxel-based statistical analysis, which explores the entire brain without predefined hypotheses, revealed CSF TDP-43 metabolic correlates in the posterior precuneus already at the prodromal (MCI) stage of AD, diagnosed based on *in vivo* biomarkers. The careful inclusion of prodromal AD patients is a deliberate feature of our study and, together with our distinct analytical approach, accounts for the divergence from earlier neuropathological reports.

Our results also deviate from (Bauer et al., 2023) who described an association of higher plasma TDP-43 levels in older adults with reduced entorhinal cortex volume and thinner cortical thickness in the cingulate/parahippocampal gyrus, suggesting these levels reflect aggregate accumulation in these regions. This discrepancy may reflect methodological differences between the studies, not only in the enrolled populations, but also on focus on morphological rather than functional/metabolic metrics and using plasma *versus* CSF TDP-43. CSF TDP-43 more directly reflects brain pathology, while plasma levels can be influenced by other peripheral factors and extra-CNS production (Araki et al., 2019; Luthi-Carter et al., 2024; Rubio et al., 2022). In fact, the potential of plasma TDP-43 as an *in vivo* proxy for aggregates remains debated (Foulds et al., 2009). The highly sensitive assay we employed was designed to detect of both full-length and truncated forms of TDP-43 levels in CSF, despite its much lower concentration than plasma (Feneberg et al., 2014). These fragments are widely recognized as a hallmark of disease in TDP-43. Under pathological conditions, TDP-43 fragments are formed into C-terminal fragments that accumulate in the cytoplasm, exposing prion-like, amyloidogenic regions. This promotes the formation of insoluble aggregates, disrupting cellular function and contributing to neurotoxicity in TDP-43 proteinopathies (López-Carbonero et al., 2024). Detecting these fragments in CSF focuses on a potential biomarker for TDP-43 pathology *in vivo*. However, their CSF concentrations may reflect a mixture of ongoing cleavage, release from degenerating neurons, and clearance mechanisms, rather than a simple read-out of aggregate burden. Also, given the ubiquitous expression of the protein, systemic stressors could in theory raise plasma TDP-43, and potentially its concentration in CSF. However, non-neurological disorders have not been definitively linked to these elevations, leaving peripheral confounding plausible yet unconfirmed. Recognition of these gaps is precisely why future validation against post-mortem immunohistochemistry will be critical. Correlating ante-mortem CSF TDP-43 levels with gold-standard neuropathological staging will ultimately determine whether these measurements can serve as a faithful *in vivo* biomarker for TDP-43 aggregates.

The literature diverges on CSF TDP-43 values measured through immunoassays in neurodegenerative diseases with some studies reporting either increased (Kapaki et al., 2022a) or decreased levels (Kuiperij et al., 2016) than controls in FTLD-TDP patients, and significantly higher levels in ALS (Kasai et al., 2009; Noto et al., 2011). These conflicting findings could stem from methodological differences and sample heterogeneity. Additionally, TDP-43 exists in multiple conformational states and localizations, ranging from soluble forms in the nucleus and cytoplasm to insoluble aggregates (Mackenzie and Neumann, 2016), complicating the interpretation of CSF levels as direct reflections of brain aggregates. Noteworthy, lower levels in ALS were linked to shorter survival, possibly indicating a higher proportion of insoluble TDP-43 forming aggregates in motor neurons (Noto et al., 2011). This observation may resemble the behavior of β-amyloid in AD CSF, where decreased levels reflect brain amyloid aggregates due to a decreased diffusion and availability in the CSF (Blennow et al., 2010). If this is the case, the positive correlation we found, where lower CSF TDP-43 levels correspond to reduced metabolism in the precuneus, could represent a downstream effect of local or distal TDP-43 aggregate pathology.

These findings raise important questions about the heterogeneity of TDP-43 pathology in AD. While some studies have suggested that TDP-43 pathology predominantly affects limbic regions (Meneses et al., 2021), our results suggest a broader network-level impact that includes posterior parietal regions, particularly the precuneus, and may also be associated with loss of connections with subcortical regions involved in the DMN. This aligns with the growing recognition of DMN nodes as sites of early vulnerability in AD (Ereira et al., 2024), emphasizing the need to consider regional specificity when studying TDP-43 proteinopathy.

The main strength of this exploratory study lies in the well-defined cohort of patients, who clinically and biologically exhibit the core characteristics of AD. Additionally, we have coupled the analysis of a CSF protein, which is still relatively unexplored in this disease, with metrics of brain metabolism. We comprised exclusively MCI-AD patients with amnestic syndrome, an ATN-positive CSF profile and posterior temporo-parietal hypometabolism on [^{18}F]FDG-PET, each confirmed by at least two years of follow-up. The primary objective was to assess the impact of TDP-43 co-proteinopathy on cerebral metabolism in AD rather than to distinguish LATE-NC from other TDP-43 proteinopathies such as FTLD-TDP, which were effectively excluded by our selection criteria. Consequently, differentiation of LATE-NC in AD from other TDP-43 pathologies fell outside the study scope. Together, these features mitigate the limitation of a relatively small sample size, which may have reduced statistical power, although all reported results still met the predefined significance thresholds. In particular, the voxel-wise threshold of $p < 0.001$ (uncorrected) is an optimal balance between type I and type II error (Lieberman and Cunningham, 2009). A stricter voxel-level FWE threshold ($p < 0.05$) would be overly conservative for [^{18}F]FDG PET due to its modest signal-to-noise ratio, especially in small samples. In every analysis we imposed a minimum cluster extent of 100 voxels and applied cluster-level family-wise error correction, steps that together limit the chance of spurious results. Our strategy aligns with prior PET studies and recommendations for automated assessment of [^{18}F]FDG PET scans (Nobili et al., 2018).

The use of the Simoa assay, which offers a highly sensitive method for measuring both full-length and truncated forms of TDP-43, enabled us to assess the potential role of CSF TDP-43 as a biomarker for TDP-43-related pathology *in vivo*. The inclusion of healthy controls in our [^{18}F]FDG PET analyses further strengthened the specificity of our findings, supporting the notion that TDP-43 pathology results in unique metabolic disruptions distinct from the classical amyloid and tau-related metabolism deficits observed in AD. However, the lack of a healthy control group for CSF TDP-43 measurements limits our ability to contextualize absolute levels. To our knowledge, no clinically validated cut-off values

have yet been published for CSF TDP-43 measured with the Simoa assay; the few thresholds reported so far are exploratory, single-center values derived with ELISA-based platforms (Bourbouli et al., 2017; Kapaki et al., 2022b) and remain unvalidated across independent cohorts. We therefore focused on the association between CSF TDP-43 and regional glucose metabolism rather than on raw concentration values. Future studies should recruit age-matched controls to establish normative ranges and strengthen biomarker validity using neuropathologic gold standards. Additionally, the cross-sectional nature of the study precludes assessing the temporal dynamics of CSF TDP-43 levels and their relationship with disease progression. Finally, while [^{18}F]FDG PET provides valuable insights into metabolic changes, it has limitations in terms of spatial resolution and sensitivity in detecting changes in certain brain regions, such as the medial temporal lobe (MTL) (Morbelli et al., 2010; Mosconi, 2005). Recent studies using synaptic density-specific tracers, such as [^{11}C]UCB-J, have shown that the distribution of these tracers mirrors that of [^{18}F]FDG in most cortical regions, except for the MTL, where [^{18}F]FDG PET data may be less reliable. This suggests posterior brain metabolic activity may provide earlier and more robust insights into AD pathology than temporal lobe changes (van Aalst et al., 2021). In any case, albeit the MT-VOI is compact, it was defined according to previous works regions (Botha et al., 2018; Buciuc et al., 2020), and contains a sufficient voxel count for mean-uptake extraction. Thus, our findings contribute to the evolving understanding of how TDP-43 pathology interacts with different brain networks in AD, highlighting the need for careful interpretation of regional metabolic changes.

We acknowledge that the absence of a pathological gold standard for the assay validation and Tau PET imaging—which would allow a more accurate distinction among AD phenotypes—represents a limitation of the current study and interpretation of our findings. Stratifying participants into typical AD, limbic-predominant, and hippocampal-sparing variants would be highly informative, especially since limbic-predominant AD has a markedly higher likelihood of TDP-43 co-pathology (Ferreira et al., 2020). Our current sample size does not allow such subdivision, but this will be an important goal for future investigations.

Future studies should employ longitudinal designs, larger cohorts, and multimodal imaging to clarify the relationship between TDP-43 pathology, metabolic changes, and cognitive decline. Developing assays to distinguish full-length and truncated TDP-43 forms could enhance diagnostic accuracy, along with emerging techniques such as real-time quaking-induced conversion (RT-QuIC) to amplify TDP-43 aggregates *in vivo*. Recent studies have demonstrated the effectiveness of RT-QuIC in detecting TDP-43 seeding activity in both brain homogenates and olfactory mucosa of FTLD patients (Fontana et al., 2024; Scialò et al., 2020). Applying these advances to AD could enable *in vivo* imaging comparisons between TDP-43-positive and -negative patients, complementing the evidence from post-mortem studies (Buciuc et al., 2020; Lavrova et al., 2024). Until such techniques become widely available, voxel-based analysis of [^{18}F]FDG-PET scans remains a valuable tool for exploring the relationships between CSF TDP-43 levels and regional metabolic variations. This aligns with its established use in examining the metabolic correlates of several fluid biomarkers (Massa et al., 2024, 2022). This approach, though indirectly, offers insights into the pathophysiological changes in prodromal AD patients, independent of the core neuropathological features such as amyloidosis and tauopathy.

5. Conclusions

In summary, our findings suggest that TDP-43 pathology, as reflected by CSF TDP-43 levels measured with a highly sensitive immunoassay, may relate with unique metabolic disruptions in the posterior parietal regions distinct from the amyloid- and tau-related deficits typically observed in AD. In the absence of validated imaging techniques capable of precisely mapping protein aggregates beyond amyloid plaques and NFT in brain regions, our findings provide indirect insights *in vivo* into TDP-43 co-pathology in prodromal AD, affecting the functioning of cortical areas crucial for cognition. Future longitudinal studies with larger cohorts and the inclusion of healthy controls are necessary to enhance our understanding of TDP-43 as a biomarker and its role as a pathological contributor to the progression and heterogeneity of AD.

CRediT authorship contribution statement

Virginia Pelagotti: Writing – review & editing, Writing – original draft, Methodology, Investigation, Formal analysis, Data curation. **Domenico Plantone:** Writing – review & editing, Writing – original draft, Resources, Investigation, Data curation, Methodology. **Francesca D'Amico:** Investigation, Data curation, Writing – review & editing. **Stefano Raffa:** Data curation, Writing – review & editing. **Pietro Mattioli:** Writing – review & editing. **Beatrice Orso:** Writing – review & editing, Data curation. **Mattia Losa:** Writing – review & editing. **Carlo Manco:** Writing – original draft, Resources, Conceptualization, Writing – review & editing, Data curation, Supervision, Methodology. **Delia Righi:** Formal analysis, Writing – review & editing, Methodology, Data curation. **Dario Arnaldi:** Writing – review & editing, Conceptualization, Supervision. **Antonio Uccelli:** Supervision, Writing – review & editing, Resources. **Andrea Chincarini:** Formal analysis, Writing – review & editing. **Gianmario Sambuceti:** Supervision, Resources, Writing – review & editing, Methodology. **Silvia Morbelli:** Supervision, Writing – review & editing, Formal analysis, Resources. **Nicola De Stefano:** Resources, Supervision, Writing – review & editing. **Federico Massa:** Writing – review & editing, Writing – original draft, Resources, Data curation, Supervision, Methodology, Formal analysis, Software, Investigation. **Matteo Pardini:** Writing – review & editing, Validation, Supervision, Methodology, Formal analysis, Conceptualization.

Ethics approval

Written consent for anonymized data use was obtained from all subjects, adhering to university hospital rules and Helsinki Declaration principles. The study was approved by the local Ethical committee (PNRR-POC-2022-12376726).

Provenance and peer review

Not commissioned; externally peer reviewed.

Funding

This work was partially supported by a grant from the Italian Ministry of Health to IRCCS Ospedale Policlinico San Martino [Fondi per la Ricerca Corrente, and Italian Neuroscience network (RIN)] and by FRA2022/DINOGMI – Department of Neuroscience, Rehabilitation, Ophthalmology, Genetics, Maternal and Child Health, University of Genoa, and supported by #NEXTGENERATIONEU (NGEU) and funded by the Ministry of University and Research (MUR), National Recovery and Resilience Plan (NRRP), project MNESYS (PE0000006) – A Multiscale integrated approach to the study of the nervous system in health and disease (DN. 1553 11.10.2022).

Appendix A. Supplementary data

Supplementary data to this article can be found online at https://doi.org/10.1016/j.nbd.2025.107014.

Data availability

The data supporting the findings of this study are available on request from the corresponding author.

References

Albert, M.S., DeKosky, S.T., Dickson, D., Dubois, B., Feldman, H.H., Fox, N.C., Gamst, A., Holtzman, D.M., Jagust, W.J., Petersen, R.C., Snyder, P.J., Carrillo, M.C., Thies, B., Phelps, C.H., 2011. The diagnosis of mild cognitive impairment due to Alzheimer's disease: recommendations from the National Institute on Aging-Alzheimer's Association workgroups on diagnostic guidelines for Alzheimer's disease. Alzheimer's and Dementia 7, 270–279. https://doi.org/10.1016/j.jalz.2011.03.008.

Araki, K., Araki, A., Honda, D., Izumoto, T., Hashizume, A., Hijikata, Y., Yamada, S., Iguchi, Y., Hara, A., Ikumi, K., Kawai, K., Ishigaki, S., Nakamichi, Y., Tsunekawa, S., Seino, Y., Yamamoto, A., Takayama, Y., Hidaka, S., Tominaga, M., Ohara-Imaizumi, M., Suzuki, A., Ishiguro, H., Enomoto, A., Yoshida, M., Arima, H., Muramatsu, S., Sobue, G., Katsuno, M., 2019. TDP-43 regulates early-phase insulin secretion via CaV1.2-mediated exocytosis in islets. J. Clin. Invest. 129, 3578–3593. https://doi.org/10.1172/JCI124481.

Bauer, C.E., Zachariou, V., Sudduth, T.L., Van Eldik, L.J., Jicha, G.A., Nelson, P.T., Wilcock, D.M., Gold, B.T., 2023. Plasma TDP-43 levels are associated with neuroimaging measures of brain structure in limbic regions. Alzheimer's & Dementia: Diagnosis, Assessment & Disease Monitoring 15. https://doi.org/10.1002/dad2.12437.

Blennow, K., Hampel, H., Weiner, M., Zetterberg, H., 2010. Cerebrospinal fluid and plasma biomarkers in Alzheimer disease. Nat. Rev. Neurol. 6, 131–144. https://doi.org/10.1038/nrneurol.2010.4.

Botha, H., Mantyh, W.G., Murray, M.E., Knopman, D.S., Przybelski, S.A., Wiste, H.J., Graff-Radford, J., Josephs, K.A., Schwarz, C.G., Kremers, W.K., Boeve, B.F., Petersen, R.C., Machulda, M.M., Parisi, J.E., Dickson, D.W., Lowe, V., Jack, C.R., Jones, D.T., 2018. FDG-PET in tau-negative amnestic dementia resembles that of autopsy-proven hippocampal sclerosis. Brain 141, 1201–1217. https://doi.org/10.1093/brain/awy049.

Bourbouli, M., Rentzos, M., Bougea, A., Zouvelou, V., Constantinides, V.C., Zaganas, I., Evdokimidis, I., Kapaki, E., Paraskevas, G.P., 2017. Cerebrospinal fluid TAR DNA-binding protein 43 combined with tau proteins as a candidate biomarker for amyotrophic lateral sclerosis and frontotemporal dementia spectrum disorders. Dement. Geriatr. Cogn. Disord. 44, 144–152. https://doi.org/10.1159/000478979.

Braak, H., Alafuzoff, I., Arzberger, T., Kretzschmar, H., Del Tredici, K., 2006. Staging of Alzheimer disease-associated neurofibrillary pathology using paraffin sections and immunocytochemistry. Acta Neuropathol. 112, 389–404. https://doi.org/10.1007/s00401-006-0127-z.

Buciuc, M., Botha, H., Murray, M.E., Schwarz, C.G., Senjem, M.L., Jones, D.T., Knopman, D.S., Boeve, B.F., Petersen, R.C., Jack, C.R., Petrucelli, L., Parisi, J.E., Dickson, D.W., Lowe, V., Whitwell, J.L., Josephs, K.A., 2020. Utility of FDG-PET in diagnosis of Alzheimer-related TDP-43 proteinopathy. Neurology 95. https://doi.org/10.1212/WNL.0000000000009722.

Buckner, R.L., DiNicola, L.M., 2019. The brain's default network: updated anatomy, physiology and evolving insights. Nat. Rev. Neurosci. 20, 593–608. https://doi.org/10.1038/s41583-019-0212-7.

Butler Pagnotti, R.M., Pudumjee, S.B., Cross, C.L., Miller, J.B., 2023. Cognitive and clinical characteristics of patients with limbic-predominant age-related TDP-43 encephalopathy. Neurology 100. https://doi.org/10.1212/WNL.0000000000207159.

Ereira, S., Waters, S., Razi, A., Marshall, C.R., 2024. Early detection of dementia with default-mode network effective connectivity. Nature Mental Health 2, 787–800. https://doi.org/10.1038/s44220-024-00259-5.

Feneberg, E., Steinacker, P., Lehnert, S., Schneider, A., Walther, P., Thal, D.R., Linsenmeier, M., Ludolph, A.C., Otto, M., 2014. Limited role of free TDP-43 as a diagnostic tool in neurodegenerative diseases. Amyotroph Lateral Scler Frontotemporal Degener 15, 351–356. https://doi.org/10.3109/21678421.2014.905606.

Ferreira, D., Nordberg, A., Westman, E., 2020. Biological subtypes of Alzheimer disease. Neurology 94, 436–448. https://doi.org/10.1212/WNL.0000000000009058.

Fontana, E., Bongianni, M., Benussi, A., Bronzato, E., Scialo, C., Sacchetto, L., Cagnin, A., Castriciano, S., Buratti, E., Gardoni, F., Italia, M., Schreiber, A., Ferracin, C., Fiorini, M., Newell, K.L., Cracco, L., Garringer, H.J., Cecchini, M.P., Polymenidou, M., Padovani, A., Monaco, S., Legname, G., Ghetti, B., Borroni, B., Zanusso, G., 2024. Detection of TDP-43 seeding activity in the olfactory mucosa from patients with frontotemporal dementia. Alzheimers Dement. 20, 1156–1165. https://doi.org/10.1002/alz.13541.

Foulds, P.G., Davidson, Y., Mishra, M., Hobson, D.J., Humphreys, K.M., Taylor, M., Johnson, N., Weintraub, S., Akiyama, H., Arai, T., Hasegawa, M., Bigio, E.H., Benson, F.E., Allsop, D., Mann, D.M.A., 2009. Plasma phosphorylated-TDP-43 protein levels correlate with brain pathology in frontotemporal lobar degeneration. Acta Neuropathol. 118, 647–658. https://doi.org/10.1007/s00401-009-0594-0.

Frisoni, G.B., Festari, C., Massa, F., Cotta Ramusino, M., Orini, S., Aarsland, D., Agosta, F., Babiloni, C., Borroni, B., Cappa, S.F., Frederiksen, K.S., Froelich, L., Garibotto, V., Haliassos, A., Jessen, F., Kamondi, A., Kessels, R.P.C., Morbelli, S.D., O'Brien, J.T., Otto, M., Perret-Liaudet, A., Pizzini, F.B., Vandenbulcke, M., Vanninen, R., Verhey, F., Vernooij, M.W., Yousry, T., Boada Rovira, M., Dubois, B., Georges, J., Hansson, O., Ritchie, C.W., Scheltens, P., van der Flier, W.M., Nobili, F., 2024. European intersocietal recommendations for the biomarker-based diagnosis of neurocognitive disorders. Lancet Neurol. 23, 302–312. https://doi.org/10.1016/S1474-4422(23)00447-7.

Jack, C.R., Bennett, D.A., Blennow, K., Carrillo, M.C., Dunn, B., Haeberlein, S.B., Holtzman, D.M., Jagust, W., Jessen, F., Karlawish, J., Liu, E., Molinuevo, J.L., Montine, T., Phelps, C., Rankin, K.P., Rowe, C.C., Scheltens, P., Siemers, E., Snyder, H.M., Sperling, R., Elliott, C., Masliah, E., Ryan, L., Silverberg, N., 2018. NIA-AA research framework: toward a biological definition of Alzheimer's disease. Alzheimer's and Dementia. https://doi.org/10.1016/j.jalz.2018.02.018.

Josephs, K.A., Dickson, D.W., Tosakulwong, N., Weigand, S.D., Murray, M.E., Petrucelli, L., Liesinger, A.M., Senjem, M.L., Spychalla, A.J., Knopman, D.S., Parisi, J.E., Petersen, R.C., Jack, C.R., Whitwell, J.L., 2017. Rates of hippocampal atrophy and presence of post-mortem TDP-43 in patients with Alzheimer's disease: a longitudinal retrospective study. Lancet Neurol. 16, 917–924. https://doi.org/10.1016/S1474-4422(17)30284-3.

Kapaki, E., Boufidou, F., Bourbouli, M., Pyrgelis, E.-S., Constantinides, V.C., Anastassopoulou, C., Paraskevas, G.P., 2022a. Cerebrospinal fluid biomarker profile in TDP-43-related genetic frontotemporal dementia. J Pers Med 12, 1747. https://doi.org/10.3390/jpm12101747.

Kapaki, E., Boufidou, F., Bourbouli, M., Pyrgelis, E.-S., Constantinides, V.C., Anastassopoulou, C., Paraskevas, G.P., 2022b. Cerebrospinal fluid biomarker profile in TDP-43-related genetic frontotemporal dementia. J Pers Med. https://doi.org/10.3390/jpm12101747.

Kasai, T., Tokuda, T., Ishigami, N., Sasayama, H., Foulds, P., Mitchell, D.J., Mann, D.M. A., Allsop, D., Nakagawa, M., 2009. Increased TDP-43 protein in cerebrospinal fluid of patients with amyotrophic lateral sclerosis. Acta Neuropathol. 117, 55–62. https://doi.org/10.1007/s00401-008-0456-1.

Kreshpa, W., Raffa, S., Girtler, N., Brugnolo, A., Mattioli, P., Orso, B., Calizzano, F., Arnaldi, D., Peira, E., Chincarini, A., Tagliafico, L., Monacelli, F., Calcagno, P., Serafini, G., Gotta, F., Mandich, P., Pretta, S., Del Sette, M., Sofia, L., Sambuceti, G., Morbelli, S., Schenone, A., Massa, F., Pardini, M., 2024. Limbic network derangement mediates unawareness of apathy in mild cognitive impairment due to Alzheimer's disease: clues from [18F]FDG PET voxel-wise analysis. J. Alzheimers Dis. 101, 475–485. https://doi.org/10.3233/JAD-240430.

Kuiperij, H.B., Versleijen, A.A.M., Beenes, M., Verwey, N.A., Benussi, L., Paterlini, A., Binetti, G., Teunissen, C.E., Raaphorst, J., Schelhaas, H.J., Küsters, B., Pijnenburg, Y. A.L., Ghidoni, R., Verbeek, M.M., 2016. Tau rather than TDP-43 proteins are potential cerebrospinal fluid biomarkers for frontotemporal lobar degeneration subtypes: a pilot study. J. Alzheimers Dis. 55, 585–595. https://doi.org/10.3233/JAD-160386.

Lavrova, A., Pham, N.T.T., Vernon, C.J., Carlos, A.F., Petersen, R.C., Dickson, D.W., Lowe, V.J., Jack, C.R., Whitwell, J.L., Josephs, K.A., 2024. A multimodal clinical diagnostic approach using MRI and 18F-FDG-PET for antemortem diagnosis of TDP-43 in cases with low–intermediate Alzheimer's disease neuropathologic changes and primary age-related tauopathy. J. Neurol. 271, 4105–4118. https://doi.org/10.1007/s00415-024-12312-5.

Lee, D.S., Kang, H., Kim, H., Park, H., Oh, J.S., Lee, J.S., Lee, M.C., 2008. Metabolic connectivity by interregional correlation analysis using statistical parametric mapping (SPM) and FDG brain PET; methodological development and patterns of metabolic connectivity in adults. Eur. J. Nucl. Med. Mol. Imaging 35, 1681–1691. https://doi.org/10.1007/s00259-008-0808-z.

Lieberman, M.D., Cunningham, W.A., 2009. Type I and type II error concerns in fMRI research: re-balancing the scale. Soc. Cogn. Affect. Neurosci. 4, 423–428. https://doi.org/10.1093/scan/nsp052.

López-Carbonero, J.I., García-Toledo, I., Fernández-Hernández, L., Bascuñana, P., Gil-Moreno, M.J., Matías-Guiu, J.A., Corrochano, S., 2024. In vivo diagnosis of TDP-43 proteinopathies: in search of biomarkers of clinical use. Transl Neurodegener 13, 29. https://doi.org/10.1186/s40035-024-00419-8.

Luthi-Carter, R., Cappelli, S., Le Roux-Bourdieu, M., Tentillier, N., Quinn, J.P., Petrozziello, T., Gopalakrishnan, L., Sethi, P., Choudhary, H., Bartolini, G., Gebara, E., Stuani, C., Font, L., An, J., Ortega, V., Sage, J., Kosa, E., Trombetta, B.A., Simeone, R., Seredenina, T., Afroz, T., Berry, J.D., Arnold, S.E., Carlyle, B.C., Adolfsson, O., Sadri-Vakili, G., Buratti, E., Bowser, R., Agbas, A., 2024. Location and function of TDP-43 in platelets, alterations in neurodegenerative diseases and arising considerations for current plasma biobank protocols. Sci. Rep. 14, 21837. https://doi.org/10.1038/s41598-024-70822-8.

Mackenzie, I.R.A., Neumann, M., 2016. Molecular neuropathology of frontotemporal dementia: insights into disease mechanisms from postmortem studies. J. Neurochem. 138, 54–70. https://doi.org/10.1111/jnc.13588.

Massa, F., Grisanti, S., Brugnolo, A., Doglione, E., Orso, B., Morbelli, S., Bauckneht, M., Origone, P., Filippi, L., Arnaldi, D., De Carli, F., Pardini, M., Pagani, M., Nobili, F., Girtler, N., 2020. The role of anterior prefrontal cortex in prospective memory: an exploratory FDG-PET study in early Alzheimer's disease. Neurobiol. Aging 96, 117–127. https://doi.org/10.1016/j.neurobiolaging.2020.09.003.

Massa, F., Halbgebauer, S., Barba, L., Oeckl, P., de San, Gómez, José, N., Bauckneht, M., Lanfranchi, F., Vigo, T., Arnaldi, D., Pardini, M., Morbelli, S., Chincarini, A., Barthel, H., Otto, M., Nobili, F., 2022. Exploring the brain metabolic correlates of process-specific CSF biomarkers in patients with MCI due to Alzheimer's disease: preliminary data. Neurobiol. Aging 117, 212–221. https://doi.org/10.1016/j.neurobiolaging.2022.03.019.

Massa, F., Martinuzzo, C., de San, Gómez, José, N., Pelagotti, V., Kreshpa, W., Abu-Rumeileh, S., Barba, L., Mattioli, P., Orso, B., Brugnolo, A., Girtler, N., Vigo, T., Arnaldi, D., Serrati, C., Uccelli, A., Morbelli, S., Chincarini, A., Otto, M., Pardini, M., 2024. Cerebrospinal fluid NPTX2 changes and relationship with regional brain metabolism metrics across mild cognitive impairment due to Alzheimer's disease. J. Neurol. 271, 1999–2009. https://doi.org/10.1007/s00415-023-12154-7.

Matsuda, H., 2001. Cerebral blood flow and metabolic abnormalities in Alzheimer's disease. Ann. Nucl. Med. 15, 85–92. https://doi.org/10.1007/BF02988596.

Meneses, A., Koga, S., O'Leary, J., Dickson, D.W., Bu, G., Zhao, N., 2021. TDP-43 pathology in Alzheimer's disease. Mol. Neurodegener. 16, 84. https://doi.org/10.1186/s13024-021-00503-x.

Morbelli, S., Piccardo, A., Villavecchia, G., Dessi, B., Brugnolo, A., Piccini, A., Caroli, A., Frisoni, G., Rodriguez, G., Nobili, F., 2010. Mapping brain morphological and

functional conversion patterns in amnestic MCI: a voxel-based MRI and FDG-PET study. Eur. J. Nucl. Med. Mol. Imaging 37, 36–45. https://doi.org/10.1007/s00259-009-1218-6.

Morbelli, S., Brugnolo, A., Bossert, I., Buschiazzo, A., Frisoni, G.B., Galluzzi, S., van Berckel, B.N.M., Ossenkoppele, R., Perneczky, R., Drzezga, A., Didic, M., Guedj, E., Sambuceti, G., Bottoni, G., Arnaldi, D., Picco, A., De Carli, F., Pagani, M., Nobili, F., 2015. Visual versus semi-quantitative analysis of 18F-FDG-PET in amnestic MCI: an European Alzheimer's disease consortium (EADC) project. J. Alzheimers Dis. 44, 815–826. https://doi.org/10.3233/JAD-142229.

Mosconi, L., 2005. Brain glucose metabolism in the early and specific diagnosis of Alzheimer's disease. Eur. J. Nucl. Med. Mol. Imaging 32, 486–510. https://doi.org/10.1007/s00259-005-1762-7.

Nelson, P.T., Dickson, D.W., Trojanowski, J.Q., Jack, C.R., Boyle, P.A., Arfanakis, K., Rademakers, R., Alafuzoff, I., Attems, J., Brayne, C., Coyle-Gilchrist, I.T.S., Chui, H. C., Fardo, D.W., Flanagan, M.E., Halliday, G., Hokkanen, S.R.K., Hunter, S., Jicha, G. A., Katsumata, Y., Kawas, C.H., Keene, C.D., Kovacs, G.G., Kukull, W.A., Levey, A.I., Makkinejad, N., Montine, T.J., Murayama, S., Murray, M.E., Nag, S., Rissman, R.A., Seeley, W.W., Sperling, R.A., White III, C.L., Yu, L., Schneider, J.A., 2019. Limbic-predominant age-related TDP-43 encephalopathy (LATE): consensus working group report. Brain 142, 1503–1527. https://doi.org/10.1093/brain/awz099.

Neumann, M., Lee, E.B., Mackenzie, I.R., 2021. Frontotemporal Lobar Degeneration TDP-43-Immunoreactive Pathological Subtypes: Clinical and Mechanistic Significance, pp. 201–217. https://doi.org/10.1007/978-3-030-51140-1_13.

Nobili, F., Festari, C., Altomare, D., Agosta, F., Orini, S., Van Laere, K., Arbizu, J., Bouwman, F., Drzezga, A., Nestor, P., Walker, Z., Boccardi, M., 2018. Automated assessment of FDG-PET for differential diagnosis in patients with neurodegenerative disorders. Eur. J. Nucl. Med. Mol. Imaging. https://doi.org/10.1007/s00259-018-4030-3.

Noto, Y.-I., Shibuya, K., Sato, Y., Kanai, K., Misawa, S., Sawai, S., Mori, M., Uchiyama, T., Isose, S., Nasu, S., Sekiguchi, Y., Fujimaki, Y., Kasai, T., Tokuda, T., Nakagawa, M., Kuwabara, S., 2011. Elevated CSF TDP-43 levels in amyotrophic lateral sclerosis: specificity, sensitivity, and a possible prognostic value. Amyotroph. Lateral Scler. 12, 140–143. https://doi.org/10.3109/17482968.2010.541263.

Rolls, E.T., Wirth, S., Deco, G., Huang, C., Feng, J., 2023. The human posterior cingulate, retrosplenial, and medial parietal cortex effective connectome, and implications for memory and navigation. Hum. Brain Mapp. 44, 629–655. https://doi.org/10.1002/hbm.26089.

Rubio, M.A., Herrando-Grabulosa, M., Velasco, R., Blasco, I., Povedano, M., Navarro, X., 2022. TDP-43 cytoplasmic translocation in the skin fibroblasts of ALS patients. Cells. https://doi.org/10.3390/cells11020209.

Scialò, C., Tran, T.H., Salzano, G., Novi, G., Caponnetto, C., Chiò, A., Calvo, A., Canosa, A., Moda, F., Caroppo, P., Silani, V., Ticozzi, N., Ratti, A., Borroni, B., Benussi, L., Ghidoni, R., Furlanis, G., Manganotti, P., Senigagliesi, B., Parisse, P., Brasselet, R., Buratti, E., Legname, G., 2020. TDP-43 real-time quaking induced conversion reaction optimization and detection of seeding activity in CSF of amyotrophic lateral sclerosis and frontotemporal dementia patients. Brain Commun 2. https://doi.org/10.1093/braincomms/fcaa142.

Seoane, S., van den Heuvel, M., Acebes, Á., Janssen, N., 2024. The subcortical default mode network and Alzheimer's disease: a systematic review and meta-analysis. Brain Commun 6. https://doi.org/10.1093/braincomms/fcae128.

Tomé, S.O., Gomes, L.A., Li, X., Vandenberghe, R., Tousseyn, T., Thal, D.R., 2021. TDP-43 interacts with pathological τ protein in Alzheimer's disease. Acta Neuropathol. 141, 795–799. https://doi.org/10.1007/s00401-021-02295-2.

van Aalst, J., Ceccarini, J., Sunaert, S., Dupont, P., Koole, M., Van Laere, K., 2021. In vivo synaptic density relates to glucose metabolism at rest in healthy subjects, but is strongly modulated by regional differences. J. Cereb. Blood Flow Metab. 41, 1978–1987. https://doi.org/10.1177/0271678X20981502.